

Relative importance of crystal field versus bandwidth to the high pressure spin transition in transition metal monoxides

Luke Shulenburger,¹ Sergej Yu Savrasov² and R E Cohen^{1,3}

¹ Geophysical Laboratory, Carnegie Institution of Washington, 5251 Broad Branch Rd, NW, Washington, D. C. 20015, USA

² Department of Physics, University of California at Davis, One Shields Ave, Davis, CA 95616, USA

E-mail: lshulenburger@ciw.edu

Abstract. The crystal field splitting and d bandwidth of the $3d$ transition metal monoxides MnO, FeO, CoO and NiO are analyzed as a function of pressure within density functional theory. In all four cases the $3d$ bandwidth is significantly larger than the crystal field splitting over a wide range of compressions. The bandwidth actually increases more as pressure is increased than the crystal field splitting. Therefore the role of increasing bandwidth must be considered in any explanation of a possible spin collapse that these materials may exhibit under pressure.

1. Introduction

At low pressures the $3d$ transition metal oxides (TMOs) are magnetic and high spin. The existence and nature of a high spin to low spin transition for these materials at high pressure has been discussed widely in the literature. The earliest theoretical studies of the system with density functional theory (DFT) predicted that magnetic moments on the metal ions switch to a much smaller value at experimentally accessible pressures[1]. Subsequent experiments claimed to confirm this prediction[2] only to be contradicted by later experiments and more refined electronic structure calculations[3; 4].

The question of the mechanism for the spin collapse in $3d$ transition metal oxides has recently been revisited, with differing conclusions from dynamical mean field theory[5] and a model fit to experimental results[6]. These papers explain the spin transition in terms of the crystal field splitting and the $3d$ bandwidth with Kunes et al. arguing for the crystal field splitting driving the transition and Mattila et al. suggesting that there is a competition between the crystal field splitting and the bandwidth. We address this situation by calculating the crystal field splitting and $3d$ bandwidth for four TMOs as a function of pressure within DFT[7].

To drive a spin collapse via the crystal field splitting, the decreased exchange energy available to electrons in a high spin configuration must be offset by the change in the single particle energy levels due to the crystal field splitting. The effect of pressure on the exchange energy is small whereas the crystal field splitting does significantly change the energy of the d orbitals as the

³ This paper was presented by R.E.C. as a part of the invited talk entitled “Quantum Monte Carlo Simulations of Behavior at Extreme Conditions”

material is compressed. Typically the crystal field splitting is treated as being dominated by the electrostatic interaction of the neighboring oxygen atoms with the metal sites. However, a much greater effect is the increasing overlap and subsequent hybridization of the oxygen 2p states with the metal 3d states[3]. This change in single particle energy levels favors the pairing of the d electrons in the lower energy d orbitals, resulting in a reduced magnetic moment.

The other explanation for the spin collapse is that as the pressure is increased, the band energy sacrificed to break symmetry and form a magnetic state eventually becomes larger than the energy to be gained by the magnetic interaction. This competition can be analyzed in light of the extended Stoner theory of magnetism[8; 9] which allows these competing effects to be quantified. The extended Stoner theory works equally well for ordered and disordered magnetic states and can predict the optimal magnetic moment in contrast to the simple Stoner model that only determines if an instability to magnetism exists. The essential ingredients to this analysis are the change in the interaction energy with respect to magnetic moment and the change in magnetism with respect to the exchange splitting. Both of these quantities are driven by a change in the bandwidth near the Fermi level, which in this case is the 3d bandwidth. In this case an increase in the bandwidth will raise the energy necessary to form a high spin state, eventually causing a transition to a low spin state.

2. Methodology

We compare these mechanisms by studying an idealized system with a purely cubic structure at zero temperature in order to isolate the electronic contributions to the phenomenon (there is significant magnetoelastic coupling in the real monoxides[10]). Despite the well known failings of DFT withing the local density approximation to capture properties such as band gap of the TMOs, it is nonetheless useful for gaining a qualitative intuition into the physics of these materials. Additionally, nonmagnetic LDA is the typical starting point for both the LDA+U [11; 12] and LDA+DMFT[13] approaches, giving a special importance to the details of this solution. We will also comment on how the strong correlations present affect these quantities by examining LDA+U results.

We use a full potential linear muffin tin orbital (LMTO) method, that allows the results of the DFT calculations to be transformed directly into a tight binding Hamiltonian with no approximations[14]. In this tight binding approach, we consider a set of atomic-like wavefunctions centered on the ions where the each state has energy

$$\epsilon_\alpha = \langle \Psi_\alpha | \hat{H} | \Psi_\alpha \rangle \quad (1)$$

and states are coupled by hopping matrix elements

$$t_{\alpha,\beta} = \langle \Psi_\alpha | \hat{H} | \Psi_\beta \rangle \quad (2)$$

where \hat{H} is an effective Hamiltonian determined from the results of the DFT calculation.

3. Results and Discussion

As a first application of this technique, we consider the on site energies of the oxygen 2p orbitals and metal 3d state in Fig.1. The plot shows that as the number of electrons in the problem is increased, the energy gap between the oxygen and metal 3d states decreases and the hopping between those states also becomes less favorable.

These calculations also provide estimates of the crystal field splitting and d bandwidth in the TMOs as a function of pressure, determining the relative size of these terms and how they behave under pressure. In this case the bands near the Fermi energy that are important to the low energy physics of the system are formed by the hybridization of the metal 3d orbitals

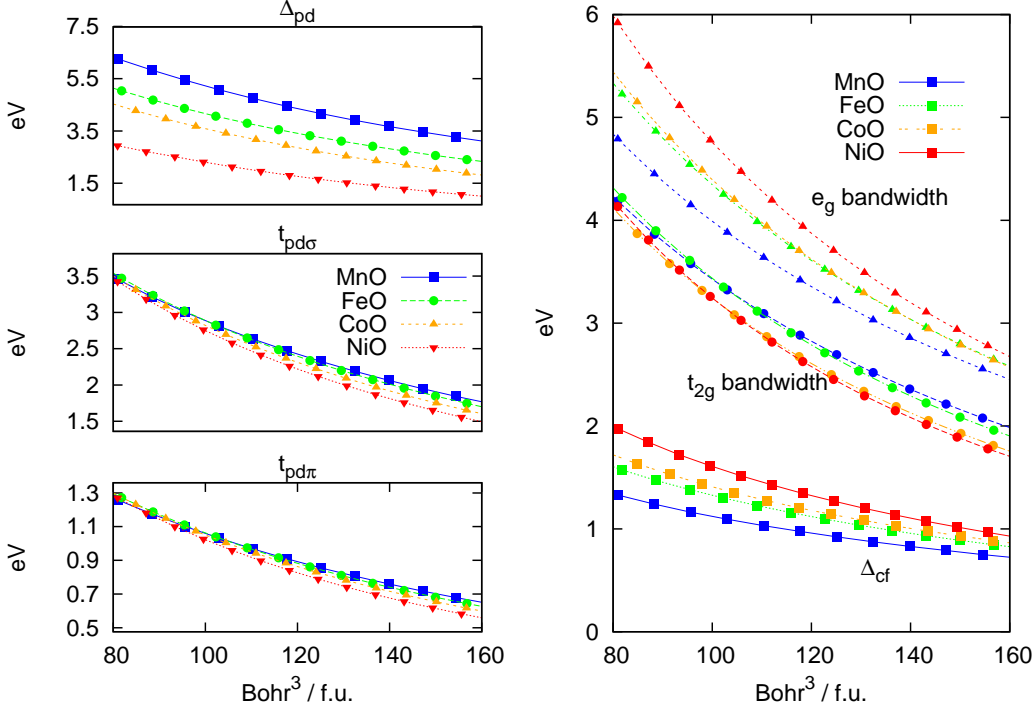


Figure 1. Left: Derived tight-binding Hamiltonian elements for the transition metal oxides versus the functional unit volume (one metal ion and one oxygen). Δ_{pd} is the energy difference between the $3d e_g$ orbital and the corresponding oxygen $2p$ orbital. Two hopping matrix elements are also shown. $t_{pd\sigma}$ connects the t_{2g} orbitals with the oxygen $2p$ orbitals parallel to the line connecting the metal and the oxygen. Likewise $t_{pd\pi}$ connects the t_{2g} orbitals with oxygen $2p$ orbitals perpendicular to the line connecting the metal and the oxygen. Right: Derived tight-binding bandwidth and crystal field splitting for nonmagnetic TMOs via LDA calculations as a function of cell volume. The squares indicate crystal field splitting, the circles the t_{2g} bandwidth and the triangles the e_g bandwidth

with the surrounding oxygen $2p$ orbitals. For the cubic NaCl structure, there are two different symmetries of d-orbital to be considered. The first are the two e_g orbitals that point towards the nearest neighbor oxygen atoms. These orbitals form bands that are raised in energy versus the isolated d orbital because of the electrostatic interaction of the electrons on the metal ion with the negatively charged O ion as well as the hybridization of the p and d orbitals. The second class of orbital which is of interest are the three t_{2g} orbitals that do not point towards the nearest neighbor oxygens. These orbitals will form bands which are relatively lower in energy than the e_g orbitals. The difference in energy between these two sets of orbitals is conventionally termed crystal field splitting.

To quantify the crystal field splitting and to determine the interactions that are important to these bands, it is possible to compare the results of tight binding calculations with ever larger sets of orbitals to the results of self consistent density functional calculations. In this case, it is found that the qualitative features of the bands are preserved by a Hamiltonian containing only the nearest oxygen $2p$ and metal $3d$ states. This band would be derived by solving the one dimensional tight binding matrix equation

$$\begin{pmatrix} \epsilon_d & t_{pd\sigma} \\ t_{pd\sigma} & \epsilon_p \end{pmatrix} \begin{pmatrix} \Psi_d(\vec{k}) \\ \Psi_p(\vec{k}) \end{pmatrix} = E_{e_g}(\vec{k}) \begin{pmatrix} \Psi_d(\vec{k}) \\ \Psi_p(\vec{k}) \end{pmatrix}, \quad (3)$$

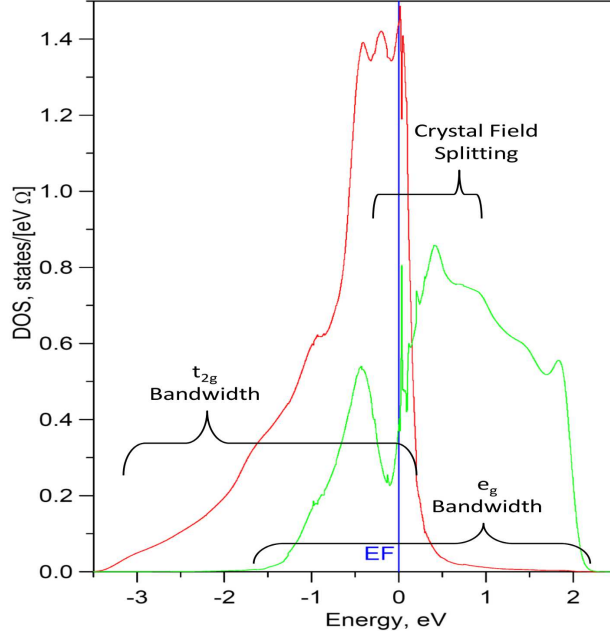


Figure 2. Partial density of states of FeO with a lattice constant of 4.0228 Angstrom from DFT LDA calculations. The total density of states is projected onto atomic d orbitals centered on the Fe atom. The bandwidths of the e_g and t_{2g} bands are indicated, as well as the crystal field splitting which is the distance between the centers of the two bands. All energies are measured in eV relative to the Fermi energy.

where the basis for the wavefunction is the proper symmetry d orbital on the metal ion and the p orbital on the nearest neighbor oxygen ions. In this case the crystal momentum \vec{k} is given along the direction connecting the metal ion and one of the nearest neighbor oxygens, which is appropriate because the band obtains both its minimum and maximum energies in this direction. Solving this equation for the lowest energy state gives an energy for the e_g band

$$E_{e_g}(\vec{k}) = \frac{\epsilon_d + \epsilon_p}{2} + \sqrt{\left(\frac{\epsilon_d - \epsilon_p}{2}\right)^2 + 4t_{pd\sigma}^2 \sin\left(\frac{\vec{k} \cdot \vec{a}}{2}\right)}, \quad (4)$$

where \vec{a} is a primitive translation vector in the same direction as \vec{k} .

For quantitative agreement in the width and location of the bands, it is necessary to include next nearest neighbor hopping between the metal ion and the fcc lattice of metal ions surrounding it. This can be done by replacing the onsite energy, ϵ_d , of the d orbital with a \vec{k} dependent band taking into account the hybridization with the next nearest neighbor metal ions. Following the work of Harrison[15] and solving a similar but larger matrix equation as in Eq. 3, this gives the following expression for the energy of the d band:

$$E_d(\vec{k}) = \epsilon_d + t_{dd\pi} + 3t_{dd\delta} + \left(\frac{t_{dd\sigma}}{2} + \frac{3t_{dd\pi}}{2} + \frac{3t_{dd\delta}}{2}\right) \cos\left(\frac{\sqrt{2}\vec{k} \cdot \vec{a}}{2}\right) \quad (5)$$

Substituting this k dependent energy of the d band into Eq. 4, the full energy dependence of the

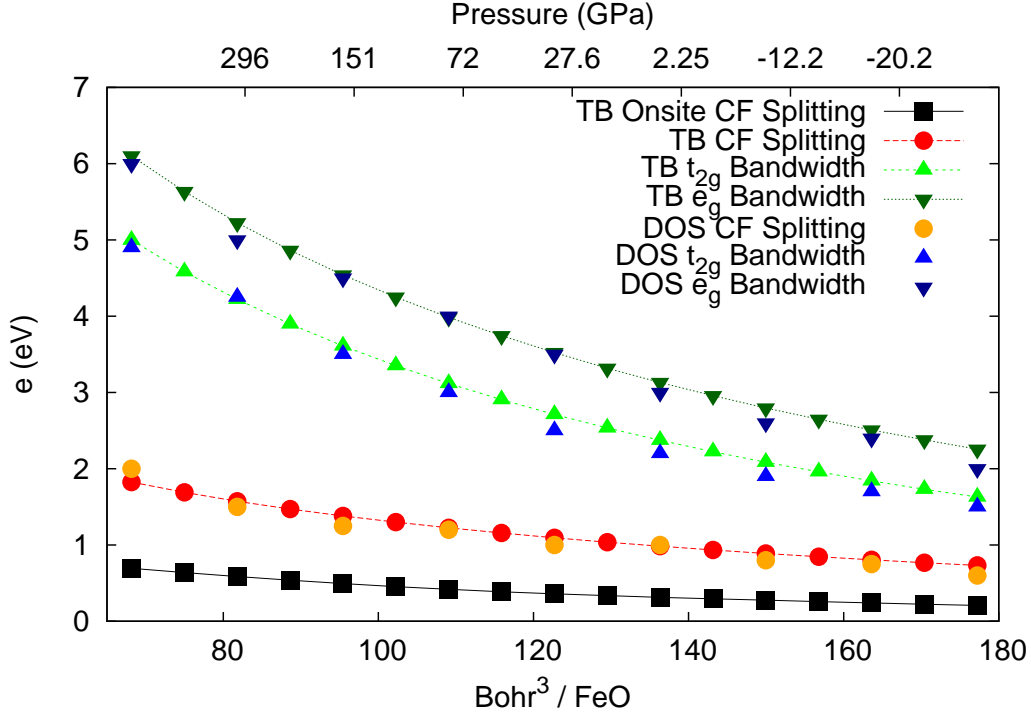


Figure 3. Crystal field splitting and $3d$ bandwidth of FeO from tight binding and the density of states. The black squares are the crystal field splitting from the on site terms in the tight binding. Points connected with lines are from the tight binding expressions. All quantities are plotted as a function of the volume of the cell containing one FeO pair. The pressures indicated on the top axis are from a Vinet equation of state fit to the antiferromagnetic LDA+U energies.

e_g band including next nearest neighbor interactions is

$$E_{e_g}(\vec{k}) = \frac{E_d(\vec{k}) + \epsilon_p}{2} + \sqrt{\left(\frac{E_d(\vec{k}) - \epsilon_p}{2}\right)^2 + 4t_{pd\sigma}^2 \sin^2\left(\frac{\vec{k} \cdot \vec{a}}{2}\right)} \quad (6)$$

A similar expression can be obtained for the t_{2g} band, first substituting $t_{pd\pi}$ for $t_{pd\sigma}$ in Eq. 6 and using the appropriate matrix elements for the second nearest neighbor $d-d$ interaction in Eq. 5. Using these expressions in Eqs. 5 and 6, the bandwidth is the difference between the extremes of Eq. 6 and the crystal field splitting is the difference between the center of mass of the e_g and t_{2g} bands. With this prescription, the bandwidth and crystal field splitting of the transition metal oxides as a function of lattice constant is shown on the right side of Fig. 1

In order to check the validity of these tight binding results, we calculate the bandwidth and crystal field splitting of FeO using both the tight binding approximation and the partial density of states. For the partial density of states, the d bandwidth is simply the spread of the density of states projected onto the $3d$ orbitals with the same symmetry as the band in question. The crystal field splitting is determined by the distance between the center of mass of the two independent $3d$ bands. These quantities are illustrated for the partial density of states of FeO as shown in Fig. 2.

The agreement between these two methods is excellent as shown in Fig. 3. This figure also shows that the crystal field splitting is not simply due to a change in the energy of the various $3d$ orbitals on the metal ion. This result is somewhat surprising given the seminal work of

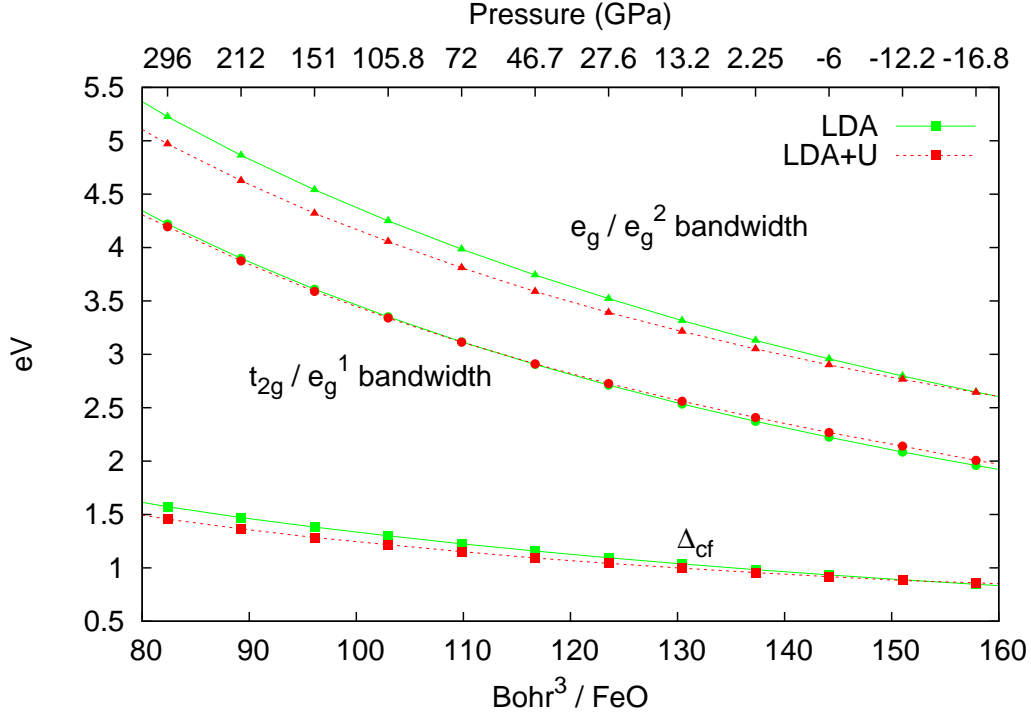


Figure 4. Comparison of bandwidth and crystal field splitting obtained via nonmagnetic LDA and antiferromagnetic LDA+U calculations as a function of compression. The squares indicate crystal field splitting, the circles the t_{2g} bandwidth and the triangles the e_g bandwidth. The LDA results are plotted in green and connected by solid lines and the LDA+U results are plotted in red and connected by dotted lines. The pressures are from a Vinet equation fit to the LDA+U energies.

Mattheiss who showed from symmetry arguments that the crystal field splitting at the gamma point is due entirely to hopping between nearest neighbor metal ions with no effect due to the oxygen[16; 17]. This seeming inconsistency is resolved by noting that the full crystal field splitting is an average over the full Brillouin zone rather than being defined by the behavior at the gamma point. Indeed, the Mattheiss result is not incompatible with our tight binding framework. In tight binding calculations, the hopping matrix element between the O $2p$ and Fe $3d$ states can be set to zero independently with the result that the crystal field splitting at gamma is unchanged, but the full crystal field splitting is changed.

These calculations have shown that the absolute value of the $3d$ bandwidth is much greater than the crystal field splitting. Additionally, the change of this quantity with pressure is much greater than that of the the crystal field splitting. These results strongly suggest that the spin transition is not entirely due to the change of crystal field splitting with pressure, owing at least in part to the increase in the $3d$ bandwidth.

To check the robustness of this result, the crystal field splitting and $3d$ bandwidth were also calculated using LDA+U with the tight binding approach. In the antiferromagnetic ground state, the electronic symmetry is lowered from cubic to rhombohedral thus the crystal field picture is slightly changed. However, the difference between the e_g^1 state and the e_g^2 state for the minority spin of FeO at ambient pressure gives a crystal field splitting of 0.95 eV, and bandwidths of 3.05 and 2.408 eV respectively with a dependence on pressure which is very similar to that of the LDA results. This result is robust with respect to pressure, as shown for FeO in Fig. 4, showing

that addition of the magnetism and strong interactions does not greatly change the nature of bonding for the 3d electrons.

4. Conclusion

We have shown that the 3d bandwidth in MnO, FeO, CoO and NiO is greater than the crystal field splitting and increases with pressure. This result is robust to the choice of LDA or LDA+U correlations for the 3d electrons. Explanations of the spin collapse in these materials should account for this increasing bandwidth as well as the change in crystal field splitting.

Acknowledgments

We wish to thank I. Mazin, H-K. Mao, S. Gramsch, and P. Ganesh for insightful discussions. L.S. and R.E.C acknowledge support in the form of NSF grants TG-MCA07S016, EAR-0738061 and EAR-0530282. The LMTO code used for the calculations was developed by Sergej Savrasov with support from NSF grant DMR-0606498.

References

- [1] Cohen R E, Mazin I and Isaak D 1997 *Science* **275** 654
- [2] Pasternak M P, Taylor R D, Jeanloz R, Li X, Nguyen J H and McCammon C A 1997 *Phys. Rev. Lett.* **79** 5046–5049
- [3] Cohen R, Fei Y, Downs R, Mazin I and Isaak D 1998 *Materials Research Society Symposium Proceedings* **499** 27–40
- [4] Badro J, Struzhkin V V, Shu J, Hemley R J, Mao H k, Kao C c, Rueff J P and Shen G 1999 *Phys. Rev. Lett.* **83** 4101–4104
- [5] Kuneš J, Lukoyanov A, Anisimov V, Scalettar R and Pickett W 2008 *Nature Materials* **7** 198–202
- [6] Mattila A, Rueff J, Badro J, Vankó G and Shukla A 2007 *Phys. Rev. Lett.* **98** 196404
- [7] Kohn W and Sham L J 1965 *Phys. Rev.* **140** A1133–A1138
- [8] Anderson O, Madsen J and Poulsen U 1977 *Physica B* **86-88** 249
- [9] Krasko G L 1987 *Phys. Rev. B* **36** 8565–8569
- [10] Kantor A P, Jacobsen S D, Kantor I Y, Dubrovinsky L S, McCammon C A, Reichmann H J and Goncharenko I N 2004 *Phys. Rev. Lett.* **93** 215502
- [11] Anisimov V I, Zaanen J and Andersen O K 1991 *Phys. Rev. B* **44** 943–954
- [12] Petukhov A G, Mazin I I, Chioncel L and Lichtenstein A I 2003 *Phys. Rev. B* **67** 153106
- [13] Held K, Nekrasov I, Keller G, Eyert V, Blümer N, McMahan A, Scalettar R, Pruschke T, Anisimov V and Vollhardt D 2006 *physica status solidi (c)* **243** 2599–2631
- [14] Andersen O K and Jepsen O 1984 *Phys. Rev. Lett.* **53** 2571–2574
- [15] Harrison W A 2004 *Elementary Electronic Structure* (World Scientific Publishing Company)
- [16] Mattheiss L F 1972 *Phys. Rev. B* **5** 290–306
- [17] Mattheiss L F 1972 *Phys. Rev. B* **5** 306–315